# Max-Planck-Institut
## für Mathematik
## in den Naturwissenschaften
## Leipzig

Global Analysis of Synchronization in
Coupled Maps

by

*Jürgen Jost and Kiran M. Kolwankar*

# Global Analysis of Synchronization in Coupled Maps

Jürgen Jost and Kiran M. Kolwankar

*Max Planck Institute for Mathematics in the Sciences, Inselstrasse 22-26, D-04103 Leipzig, Germany*

(Dated: September 20, 2004)

We introduce a new method for determining the global stability of synchronization in systems of coupled identical maps. The method is based on the study of invariant measures. We apply it here to the simplest non-trivial example, namely two symmetrically coupled tent maps. We thus identify the precise value of the coupling parameter where synchronizing and desynchronizing transitions take place.

### INTRODUCTION

Although the phenomenon of synchronization of non-linear oscillators was discovered already in 1665 by Huygens, it has received systematic attention only recently [1, 2], owing mainly to newly found applications and the understanding of nonlinear systems that we have achieved through modern methods. The field received an impetus after Pecora and Carroll [3] showed that even chaotic trajectories can synchronize. Since then the phenomenon has found applications in secure communication, coupled Josephson junctions arrays etc. Around the same time, it was observed [4] experimentally that synchronous firing of neurons was important in feature binding in neural networks. Distant groups of neurons rapidly synchronize and desynchronize as the input stimulus changes, each synchronized group representing a collection of features belonging to the same percept. Thus a systematic understanding of synchronization and desynchronization has become important in neural information processing [5–7].

As a result of these developments various coupled dynamical systems have been studied that are either continuous or discrete in time, either continuously coupled or pulse coupled etc. and different types of synchronizations have arisen such as phase synchronization or complete synchronization, etc. Coupled maps have been used to a great extent to understand synchronization in particular [8–17] and complexity in dynamical systems [18–20] systems in general. The paradigm here consists of identical individual maps, typically iterates of a functional equation like the logistic one that produce chaotic dynamics. These maps then are coupled, that is each of them computes its next state not only on the basis of its own present state but also on the basis of those other ones that it is coupled to. With appropriate conditions on the coupling strengths, the individual solution is also a solution of the collective dynamics, that is, when all the maps follow their own intrinsic dynamics synchronously, we also have a solution of the coupled dynamics. This is the simplest case of synchronization. That synchronized collective dynamics, however, need not be stable even if the individual ones are. Therefore, the study of synchronization essentially depends on a stability analysis. One

may use linear stability analysis or global stability analysis (for some recent formulations, see [21–23]). In the linear stability analysis one assumes that the synchronized state follows the same dynamics as the individual uncoupled dynamics and then studies the stability of the dynamics transverse to the synchronizing manifold. However it has been observed [24] in coupled systems with delays that the synchronized dynamics can be quite different from the individual uncoupled dynamics. For a global stability analysis, one has to guess a Lyapunov function which then gives a criterion for synchronization. Thus the linear stability takes only the local dynamics into account and it makes a restricting assumption on the synchronized dynamics. In contrast, the global stability analysis, while global, depends on the choice of the Lyapunov function and may not always give optimal criteria. In general optimal global results are difficult to obtain. In many cases numerical results indicate the global stability of the synchronized state but it is difficult to prove. Thus it is necessary to develop a method to study synchronization which goes beyond these drawbacks. That is, it should be global and should not make any reference to the synchronized dynamics. This is what we achieve in this paper. We present a new global stability method that leads to sharp results, that is, it can determine the critical value of the coupling parameter above which global synchronization occurs. In order to exhibit the principal features, we apply the method here to the simplest non-trivial case, namely two symmetrically coupled tent maps. In subsequent, more detailed work, we shall treat more general cases, like general coupling schemes, unsymmetric coupling, and, in particular, also other maps, like the logistic map, the prototypical example for the generation of chaotic behavior.

Our method uses invariant measures or stationary densities[25] to study synchronization. A stationary density is the density obtained by starting from some initial distribution of the initial conditions and letting the system evolve for a long time. Though the complete characterization of such densities can be difficult, as we demonstrate below, sometimes it is sufficient to study its support to understand synchronization and this can be easier than studying the whole measure. Clearly, this approach is inherently global. The key idea is to study the

support of the invariant measure for different coupling strengths and to determine the critical value of the coupling strength when the support shrinks to the synchronized manifold. Here we restrict ourselves to considering two coupled maps. We consider the following coupled dynamical system

$$X_{n+1} = Af(X_n) := S(X_n) \tag{1}$$

where $X = (x, y)^T$ is a 2-dim column vector, $A$ is a $2 \times 2$ coupling matrix and $f$ is a map from $\Omega = [0, 1] \times [0, 1]$ onto itself. As already mentioned, in the present paper we consider the tent map defined as:

$$f(x) = \begin{cases} 2x & 0 \le x \le 1/2 \\ 2 - 2x & 1/2 \le x \le 1 \end{cases} \tag{2}$$

Different coupling matrices are chosen.

## INVARIANT MEASURES

A measure $\mu$ is said to be invariant under a transformation $S$ if $\mu(S^{-1}(A)) = \mu(A)$ for any measurable subset $A$ of $\Omega$. For example, a Dirac measure concentrated at a fixed point of the transformation is clearly invariant. An invariant measure need not be unique as can be seen immediately from the fact that if there are several fixed points then the different Dirac measures at these fixed points as well as their linear combinations are all invariant. A natural way to obtain invariant measures is to simply iterate any measure under the transformation $S$ and take an asymptotic (weak-$\star$) limit of these iterates. For example, one may start with any Dirac measure. Our interest here is not in such singular measures as they do not sample the whole phase space. We would like to start from a distribution of initial conditions spread over the whole phase space (say uniformly) and study its evolution and what kind of asymptotic limit it leads to. This is the idea of the SRB-measures, as they are called after Sinai, Ruelle, and Bowen. For some dynamical systems, any invariant measure is singular. In such cases even if we start with a uniform density we obtain a singular measure asymptotically. However, if, for example, the map is expanding everywhere then an SRB measure is absolutely continuous w.r.t. to Lebesgue measure. Therefore here we restrict ourselves to one particular map that is expanding, namely the tent map. We want to investigate how such a density depends on the coupling strength and would like to see when its support shrinks to the synchronization manifold.

There are various ways to find invariant measures. One approach is to use the so called Frobenius-Perron operator. It is defined as:

$$\int \int_D P\rho(x', y')dx'dy' = \int \int_{S^{-1}(D)} \rho(x', y')dx'dy' \tag{3}$$

If we choose $D = [0, x] \times [0, y]$ then we get

$$P\rho(x', y')dx'dy' = \frac{\partial}{\partial x}\frac{\partial}{\partial y}\int \int_{S^{-1}(D)} \rho(x', y')dx'dy' \tag{4}$$

Our $S$ is not invertible. In fact, it has 4 disjoint parts. Let us denote them by $S_i^{-1}$, $i = 1, ..., 4$. If $X \in \Omega$, since $f$ is symmetric, we get

$$P\rho(X) = J^{-1}(X)\sum_{i=1}^{4} \rho(S_i^{-1}(X)) \tag{5}$$

where $J^{-1}(X) = |dS^{-1}(X)/dX|$.

## SYMMETRIC COUPLED MAPS

In this section we choose a symmetric dissipative coupling given by

$$A = \begin{pmatrix} a - \epsilon & \epsilon \\ \epsilon & a - \epsilon \end{pmatrix} \tag{6}$$

where $0 < \epsilon < 1$ is the coupling strength and $0 < a < 1$ is a parameter. This choice for $A$ also satisfies the constraint that the row sum is a constant. This guarantees that the synchronized solution exists.

### The case $a = 1$

With this choice of $A$ we get the following functional equation for the density.

$$\begin{aligned} P\rho(x, y) = \frac{1}{4|1 - 2\epsilon|}[&\rho(\beta x/2 - \gamma y/2, -\gamma x/2 + \beta y/2) \\ +&\rho(1 - \beta x/2 + \gamma y/2, -\gamma x/2 + \beta y/2) \\ +&\rho(\beta x/2 - \gamma y/2, 1 + \gamma x/2 - \beta y/2) \\ +&\rho(1 - \beta x/2 + \gamma y/2, 1 + \gamma x/2 - \beta y/2)] \end{aligned} \tag{7}$$

where $\gamma = \epsilon/1 - 2\epsilon$ and $\beta = 1 + \gamma$. Since we know that a point belonging to $\Omega$ does not leave $\Omega$, all the arguments of $\rho$ on the right hand side of the above equation should be between 0 and 1. This gives us four lines $0 \le \beta x/2 - \gamma y/2 \le 1$ and $0 \le -\gamma x/2 + \beta y/2 \le 1$ which bound an area, say $\Gamma$. The support of the invariant measure should be contained in $\Gamma \cap \Omega$.

In order to study the evolution of supp $\rho$ we study the iterates of $\Omega$ under $S = Af$. $f$ maps $\Omega$ onto $\Omega$. Application of $A$ then leads to the parallelogram shown in Fig. 1a. The next application of $f$ leads to Fig. 1b. We use the following convention for labeling the points throughout. A point is labeled by the same letter in its image. As a result, some points in Fig. 1b have two labels. We note that the boundary in Fig. 1b is completely determined by the part of the area in the upper right quadrant in Fig. 1a. This is essentially because $l(GI) > l(EI)$ and
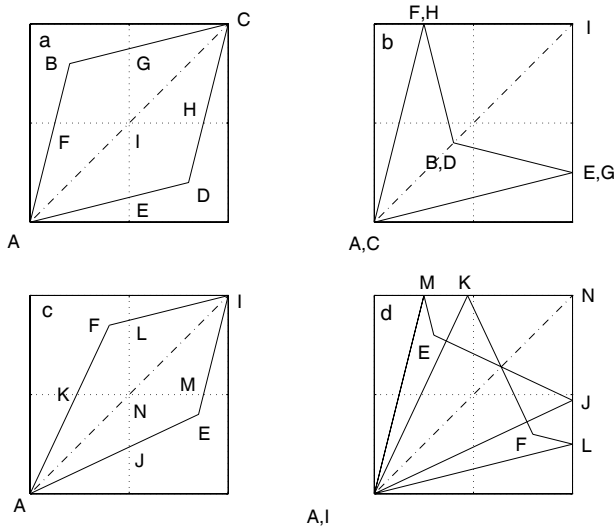
FIG. 1: The evolution of the support of the invariant measure obtained by starting from the Lebesgue measure supported on the square $[0,1] \times [0,1]$ with $\epsilon < 1/4$. a) The parallelogram ABCD obtained after the first application of $A$ b) The rhombus AFIE obtained by applying $f$ to the rectangle ABCD in a. c) The rhombus AFIE one gets when $A$ is applied to the rhombus in b. d) The next application of $f$ leads to the rhombus AMNL.

FIG. 2: The evolution of the support of the invariant measure obtained by starting from the Lebesgue measure supported on the square $[0,1] \times [0,1]$ with $\epsilon > 1/4$. a) The rhombus AFIE obtained by applying $A$ to the rhombus AFIE in Fig. 1b. b) The polygon AEMNLF one gets after the application of $f$ to the rhombus AFIE of a. c) The next application of $A$ transforms the polygon of b to this polygon AEMNLF. d) The new polygon ALOQPM obtained by the next application of $f$ to the polygon in c.

$l(HI) > l(FI)$. Let us call this *condition A*. So the areas in other quadrants get mapped inside the image of this area. Now we operate $A$ again to obtain Fig. 1c and $f$ again to get Fig. 1d. Here we have assumed that $\epsilon$ is sufficiently small so that the $x$-coordinate of F in Fig. 1c is less than $1/2$ and by symmetry the $y$-coordinate of E is less than $1/2$ (*condition B*). One can notice that, although the internal structure of the density becomes more complex, the boundary is the same as that in Fig. 1b. Also, by continuing this procedure one can see that the quadrilateral AMNL in Fig. 1d is the support of the density which remains invariant provided $\epsilon$ is sufficiently small[27].

The coordinates of F are given by

$$\begin{pmatrix} 1-\epsilon & \epsilon \\ \epsilon & 1-\epsilon \end{pmatrix} \begin{pmatrix} \frac{\epsilon}{1-\epsilon} \\ 1 \end{pmatrix} = \begin{pmatrix} 2\epsilon \\ \frac{1-2\epsilon+2\epsilon^2}{1-\epsilon} \end{pmatrix} \qquad (8)$$

As a result, the condition B leads to $\epsilon \leq 1/4$. So when $\epsilon$ satisfies this condition we get the above area as an invariant area. In [26], Pikovsky and Grassberger have made a similar observation. But our approach differs from theirs. We carry out the complete analysis using purely geometric arguments preserving the global nature of the result.

Now we have to check what happens for $\epsilon > 1/4$. So we carry out the iterations with this condition in mind. As a result in place of Fig. 1c we obtain Fig. 2a. Now if we apply $f$ we get Fig. 2b. We see that the boundary AEMNLF we obtain now is slightly different from that in Fig. 1d, the corners having been chipped off. The next application of $A$ gives us Fig. 2c. It can be easily checked
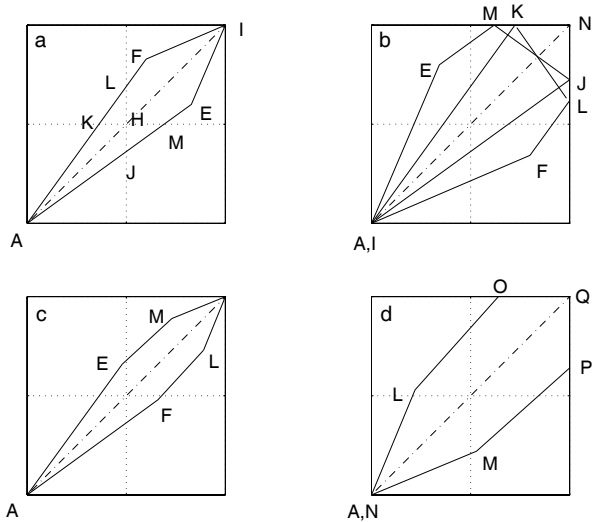
explicitly that the point E lies on the left and the point M lies on the right of the line $x = 1/2$ for any $\epsilon$ greater than $1/4$. This implies that the boundary obtained by the next application of $f$ (Fig. 2d) looks similar, that is, the number of vertices remains the same. In fact, except for the slanted portions it is exactly the same and we set out to argue that it is indeed different on those small portions. That is we cannot have a set with such a boundary as an invariant area.

In order to do this, let us first note that the magnitude of the slope of any line of the form $y = mx + c$ does not change with $f$ as it scales both axes by the same factor. And $A$ maps such a line to a new line given by

$$y = \frac{\epsilon + (1-\epsilon)m}{1-\epsilon+m\epsilon} x - \frac{\epsilon c(\epsilon + (1-\epsilon)m)}{1-\epsilon+m\epsilon} + (1-\epsilon)c \quad (9)$$

Now if the slanted portion is stable then its slope shouldn't change under $A$, so we have

$$\frac{\epsilon + (1-\epsilon)m}{1-\epsilon+m\epsilon} = m \qquad (10)$$

This implies $m^2 = 1$ ($m = 1$ in our case since we are interested in the region where both coordinates are greater than $1/2$ and $f$ does not change the slope in this region). So the slanted portion in the Fig. 2c, if it is stable, has to be of the form $y = x - (1-2\epsilon)c$. $f$ changes this intercept to $-2(1-2\epsilon)c$ and for it to be stable this should be equal to $-c$ owing to the symmetry. This implies that
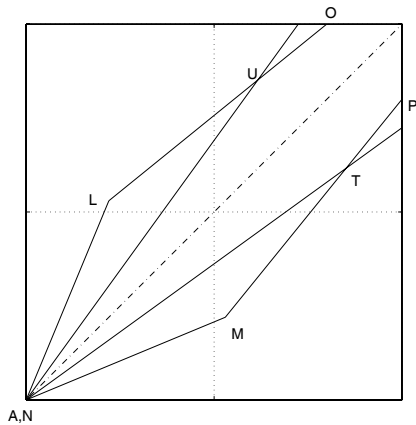
FIG. 3: This polygon would be obtained as the support of the evolving measure during the course of iterations if the condition A (see the text) was violated.



FIG. 4: The evolution of the support of the measure for the coupling matrix $A$ with general $a$. The iterates are started from the square $[0, 1] \times [0, 1]$ and $\epsilon < (2a - 1)/4$. a) The parallelogram ABCD obtained after the first application of $A$. b) The next application of $f$ transforms the parallelogram in a to this figure.

either $b = 0$ or $\epsilon = 1/4$. Therefore such a slanted portion cannot be stable for $\epsilon > 1/4$ and the whole area cannot be stable either. This shows that $\epsilon_c = 1/4$ is the critical value below which there exists an invariant area and hence no synchronization. When $\epsilon$ crosses this $\epsilon_c$ the area becomes unstable and collapses the synchronization manifold to the line $x = y$ and we get synchronization.

If the condition A is violated as well in Fig. 2c during further iterations then in that case the boundary would look something like the one shown in Fig. 3 instead of that in Fig. 2d. But since $\angle MNL > \angle EAF$, there is always a part of nonzero length of the segment $MP$ in Fig. 2c which appears as a boundary in Fig. 3 (segment MT). And then the above argument will apply to this segment.

By symmetry it can be argued that this area again becomes stable if we increase $\epsilon$ further at $\epsilon = 3/4$ and this leads to desynchronization.

It is interesting to note that the transitions of synchronization and desynchronization are discontinuous in the sense that the area of the support abruptly changes the value at the thresholds. The importance of this result lies in the fact that it is a global result.

### The case of general $a$

In this case the synchronized dynamics is different from that of the individual maps. This can be seen by taking the initial point as $X_0 = (z, z)$ which lies on the synchronization manifold which then leads to the dynamics governed by $X_{n+1} = af(X_n)$.

Now we start the iterations of $\Omega$. The first application of $A$ leads to the Fig. 4a and then $f$ maps it to Fig. 4b. One can see that if $\epsilon$ is sufficiently small so that the point $H$ remains on the left of the line $x = 1/2$ after application of $A$ then the $\angle HCG$ remains the same in the
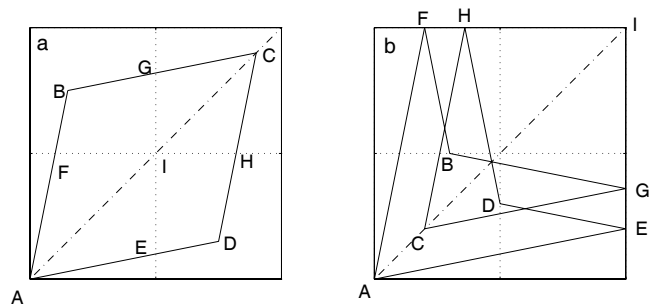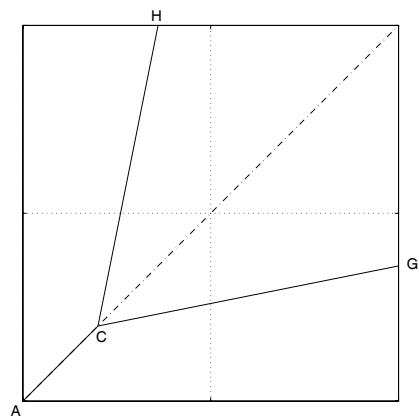


FIG. 5: The invariant area CHIG obtained asymptotically for the evolution with the coupling matrix $A$ with general $a$.

subsequent iterations whereas the $\angle FAE$ decreases with the iterations. This leads to the Fig. 5 asymptotically.

The above condition on $\epsilon$ can be calculated as for the case $a = 1$ and we get $\epsilon \leq (2a - 1)/4$. By following similar arguments as for the $a = 1$ case it can be shown that this area is unstable for $\epsilon > (2a - 1)/4$ and it reduces to the line $x = y$. Again by symmetry it can be seen that the desynchronizing transition will take place at $\epsilon = (2a + 1)/4$.

### CONCLUDING DISCUSSION

In this paper we have proposed a method that uses invariant measures and in particular their support to study synchronization. We have demonstrated it on one example, namely the tent map where we were able to study the stability of the support of the invariant measure using purely geometric arguments. In the future, different techniques to deal with invariant measures and their support will have to be developed in order for this method

to be of wide use.

While studying only the boundary of the support one has to be careful since in principle there exists a possibility that the measure can become zero asymptotically everywhere except on the synchronization manifold without making the boundary unstable. In other words, the measure can become singular. In order to avoid this situation we have considered the tent map which is expanding everywhere. But it is not sufficient to have the individual map expanding, rather it should be the coupled map that should guarantee the existence of the absolutely continuous measure. In fact, it turns out that, in all the cases considered here, the combined map ceases to be expanding exactly at the synchronization threshold. Clearly this is a consequence of the everywhere expanding property of the map chosen. While this guaranteed for us the existence of the absolutely continuous measure for $\epsilon < \epsilon_c$ and validated our use of the present method, it also raises a question as to what happens in the case of other maps and general coupling conditions. This should be clarified in future work.

In fact, one of the future directions one can explore is to try this method for different maps and also to generalize it to higher dimensions. The latter would add complications arising from the connection topologies. Various networks, such as, random, all-to-all, scale-free, small world etc. can be considered. It can be easily seen that the results of the symmetrically coupled maps would directly generalize to the all-to-all coupling owing to the symmetry. A characterization of complete measures is also needed.

---

[1] A. Pikovsky, M. Rosenblum, and J. Kurths, *Synchronization - A Universal Concept in Nonlinear Science* (Cambridge University Press, 2001).

[2] L. M. Pecora, T. L. Carroll, G. A. Johnson, D. J. Mar, and J. F. Heagy, Chaos **7**, 520 (1997).

[3] L. M. Pecora and T. L. Carroll, Phys. Rev. Lett. **64**, 821 (1990).

[4] C. M. Gray, P. König, A. K. Engel, and W. Singer, Nature **338**, 334 (1989).

[5] D. Hansel and H. Sompolinsky, Phys. Rev. Lett. **68**, 718 (1992).

[6] G. Buzsáki and A. Draguhn, Science **304**, 1926 (2004).

[7] R. W. Friedrich, C. J. Habermann, and G. Laurent, Nature Neuroscience **7**, 862 (2004).

[8] P. M. Gade, Phys. Rev. E **54**, 64 (1996).

[9] S. Jalan and R. E. Amritkar, Phys. Rev. Lett. **90**, 014101 (2003).

[10] P. Celka, Physica D **90**, 235 (1996).

[11] N. Chatterjee and N. Gupte, Phys. Rev. E **53**, 4457 (1996).

[12] Y. Maistrenko and T. Kapitaniak, Phys. Rev. E **54**, 3285 (1996).

[13] N. J. Balmforth, A. Jacobson, and A. Provenzale, Chaos **9**, 738 (1999).

[14] P. M. Gade, H. A. Cerdeira, and R. Ramaswamy, Phys. Rev. E **52**, 2478 (1995).

[15] L. Zonghua, C. Shigang, and B. Hu, Phys. Rev. E **59**, 2817 (1999).

[16] S. C. Manrubia and A. S. Mikhailov, Phys. Rev. E **60**, 1579 (1999).

[17] S. Sinha, Phys. Rev. E **66**, 016209 (2002).

[18] P. Gaspard and X.-J. Wang, Phys. Rep. **235**, 291 (1993).

[19] E. Olbrich, R. Hegger, and H. Kantz, Phys. Rev. Lett. **84**, 2132 (2000).

[20] S. D. Monte, F. d'Ovidio, H. Chate, and E. Mosekilde, Phys. Rev. Lett. **92**, 254101 (2004).

[21] L. M. Pecora and T. L. Carroll, Phys. Rev. Lett. **80**, 2109 (1998).

[22] Y. Chen, G. Rangarajan, and M. Ding, Phys. Rev. E **67**, 026209 (2003).

[23] J. Jost and M. P. Joy, Phys. Rev. E **65**, 016201 (2002).

[24] F. M. Atay, J. Jost, and A. Wende, Phys. Rev. Lett. **92**, 144101 (2004).

[25] A. Lasota and M. C. Mackey, *Chaos, Fractals and Noise* (Springer, 1994).

[26] A. Pikovsky and P. Grassberger, J. Phys. A: Math, Gen, **24**, 4587 (1991).

[27] It is not important whether we call the quadrilateral $AMNL$ in Fig. 1d an invariant area or the quadrilateral $AFIE$ in Fig. 1c since $S^n$ can also be written as $AS'^{n-1}f$ where $S' = fA$